



# Pharmacokinetic and Pharmacodynamic Profiling of Minocycline for Injection following a Single Infusion in Critically Ill Adults in a Phase IV Open-Label Multicenter Study (ACUMIN)

Thomas P. Lodise,<sup>a</sup> Scott Van Wart,<sup>b</sup> Zoe M. Sund,<sup>c</sup> Adam M. Bressler,<sup>d</sup> Akram Khan,<sup>e</sup> Amy T. Makley,<sup>f</sup> Yasir Hamad,<sup>g</sup> Robert A. Salata,<sup>h</sup> Fernanda P. Silveira,<sup>i</sup> Matthew D. Sims,<sup>j</sup> Badih A. Kabchi,<sup>k</sup> Mohamed A. Saad,<sup>l</sup> Carrie Brown,<sup>m</sup> Randolph E. Oler, Jr.,<sup>m</sup> Vance Fowler, Jr.,<sup>n</sup> Richard G. Wunderink<sup>o</sup>

<sup>a</sup>Albany College of Pharmacy and Health Sciences, Albany, New York, USA

<sup>b</sup>Enhanced Pharmacodynamics, LLC, Buffalo, New York, USA

<sup>c</sup>Duke University, Durham, North Carolina, USA

<sup>d</sup>Infectious Disease Specialists of Atlanta, Decatur, Georgia, USA

<sup>e</sup>Oregon Health and Science University, Portland, Oregon, USA

<sup>f</sup>Department of Surgery, University of Cincinnati, Cincinnati, Ohio, USA

<sup>g</sup>Department of Medicine, Washington University School of Medicine, St. Louis, Missouri, USA

<sup>h</sup>Division of Infectious Diseases and HIV Medicine, Department of Medicine, University Hospitals Cleveland Medical Center, Case Western Reserve University, Cleveland, Ohio, USA

<sup>i</sup>Department of Medicine, University of Pittsburgh Medical Center, Pittsburgh, Pennsylvania, USA

<sup>j</sup>Beaumont Hospital, Royal Oak, Michigan, USA

<sup>k</sup>Brody School of Medicine, East Carolina University, Greenville, North Carolina, USA

<sup>l</sup>University of Louisville, Louisville, Kentucky, USA

<sup>m</sup>Emmes, Rockville, Maryland, USA

<sup>n</sup>Division of Infectious Diseases, Duke University Medical Center, Durham, North Carolina, USA

<sup>o</sup>Northwestern University, Chicago, Illinois, USA

**ABSTRACT** Intravenous (i.v.) minocycline is increasingly used to treat infections caused by multidrug-resistant (MDR) *Acinetobacter baumannii*. Despite its being approved nearly 50 years ago, published information on its pharmacokinetic (PK) profile is limited. This multicenter study examined the PK and probability of pharmacokinetic-pharmacodynamic (PK-PD) target attainment profile of i.v. minocycline in critically ill patients, with suspected or documented infection with Gram-negative bacteria. The PK study population included 55 patients who received a single 200-mg i.v. dose of minocycline. Plasma PK samples were collected predose and 1, 4, 12, 24, 36, and 48 h after initiation of minocycline. Total and unbound minocycline concentrations were determined at each time point. Probabilities of achieving the PK-PD targets associated with stasis and 1-log killing (free area under the curve above the MIC [ $fAUC_{0-24h}/MIC$ ] of 12 and 18, respectively) in an immunocompetent animal pneumonia infection model of *A. baumannii* were evaluated. A two-compartment population PK model with zero-order i.v. input and first-order elimination, which estimated a constant fraction unbound ( $f_{ub}$ ) for minocycline, best characterized the total and unbound plasma minocycline concentration-time data. The only two covariates retained in the final PK model were body surface area (associated with central volume of distribution) and albumin (associated with  $f_{ub}$ ). In the PK-PD probability of target attainment analyses, minocycline 200 mg i.v. every 12 h (Q12H) was predicted to result in a suboptimal PK-PD profile for patients with *A. baumannii* infections with MIC values of  $>1$  mg/liter. Like all PK-PD profiling studies of this nature, these findings need clinical confirmation.

**Citation** Lodise TP, Van Wart S, Sund ZM, Bressler AM, Khan A, Makley AT, Hamad Y, Salata RA, Silveira FP, Sims MD, Kabchi BA, Saad MA, Brown C, Oler RE, Jr, Fowler V, Jr, Wunderink RG. 2021. Pharmacokinetic and pharmacodynamic profiling of minocycline for injection following a single infusion in critically ill adults in a phase IV open-label multicenter study (ACUMIN). *Antimicrob Agents Chemother* 65:e01809-20. <https://doi.org/10.1128/AAC.01809-20>.

**Copyright** © 2021 American Society for Microbiology. All Rights Reserved.

Address correspondence to Thomas P. Lodise, [Thomas.Lodise@acphs.edu](mailto:Thomas.Lodise@acphs.edu).

**Received** 20 August 2020

**Returned for modification** 24 September 2020

**Accepted** 24 October 2020

**Accepted manuscript posted online** 9 November 2020

**Published** 17 February 2021

**KEYWORDS** *Acinetobacter*, minocycline, pharmacodynamics, pharmacokinetics, population pharmacokinetics

*Acinetobacter baumannii* is a major cause of health care-associated infections in critically ill patients throughout the world. In recent years, a spike has occurred in the prevalence of multidrug-resistant (MDR) *A. baumannii* infections, and carbapenem-resistant *Acinetobacter* is now classified as an urgent public health threat pathogen by the CDC (1–3). Few clinically effective antimicrobials are currently available to treat MDR *A. baumannii* infections. The shortage of reliable agents has led clinicians to use classical agents like minocycline for the treatment of MDR *A. baumannii* infections (4–6). Minocycline is a semisynthetic derivative of tetracycline, has a broad spectrum of activity against Gram-positive and Gram-negative bacteria, and is approved by the FDA for the treatment of infections caused by *Acinetobacter* spp. (7, 8). Minocycline evades most tetracycline resistance mechanisms and exhibits excellent *in vitro* microbiologic activity against multidrug-resistant (MDR) *Acinetobacter baumannii* (1, 9, 10). To facilitate its use, a new formulation of minocycline (Minocin for Injection) was approved by the U.S. Food and Drug Administration (FDA) in 2015, enabling minocycline to be administered in 100 ml of normal saline over 1 h.

Although minocycline was approved nearly 50 years ago, surprisingly little is known of its pharmacokinetic (PK) and pharmacokinetic-pharmacodynamic (PK-PD) target attainment profile against *A. baumannii*. Most published PK data for intravenous (i.v.) minocycline are from healthy participant studies conducted in the 1970s that used bioassay quantification techniques (8, 11). The PK of minocycline has not been fully characterized in patients with creatinine clearance ( $CL_{CR}$ ) of  $<80$  ml/min (11), and the FDA product labeling indicates that current data are insufficient to determine if dose adjustments are warranted among patients with renal impairment (8). More importantly, it is unclear if current FDA dosing of i.v. minocycline is sufficient in achieving the critical free plasma PK-PD exposure targets associated with bacterial killing in the lung (12), especially among critically ill patients across the range of MIC values observed in *Acinetobacter* sp. encountered in clinical practice.

Given these critical gaps in the literature, this study was conducted to examine the PK of the currently marketed formulation of i.v. minocycline in critically ill patients with suspected or documented Gram-negative infections in the intensive care unit (ICU). Data obtained from this study were used to develop a population PK model to describe the PK profile of minocycline in ICU patients and to examine potential patient factors which may affect minocycline PK parameters. Monte Carlo simulations were performed with the final PK model to evaluate the PK-PD target attainment profile of i.v. minocycline against *A. baumannii* and to assess whether adjustments in the approved FDA minocycline dosing regimen are needed for critically ill adults based upon clinically relevant covariate effects.

## RESULTS

**Study population.** Disposition of study population is shown in Fig. S1 in the supplemental material. A total of 65 subjects were screened, and 58 were enrolled in the study. Out of the 58 subjects enrolled, 57 subjects (98%) received the full dose of the study product, 55 had at least 1 PK sample that was processed in accordance with specified study procedures, 52 subjects (90%) completed follow-up, 50 subjects (86%) were considered to be PK evaluable, and 49 subjects (84%) completed all PK blood draws. In the safety population, no treatment-related Serious Adverse Events (SAEs) were reported. One severe SAE (cardiopulmonary arrest resulting in death) was reported but considered unrelated to the study product. Changes in laboratory values and vital signs occurred over the 48-h observation period but were consistent with the typical variability observed in these parameters among critically ill patients.

A total of 308 unbound and 310 total plasma minocycline concentrations collected from 55 ICU patients were available for developing the population PK model. Since only

**TABLE 1** Summary statistics of baseline patient demographic, clinical laboratory, and disease-related characteristics for patients used to develop the population PK model

Variable	n (%)	Mean	SD	Median	Min	Max
Age (yr)	55	61.7	15.1	63.0	23	89
Wt (kg)	55	93.3	33.3	87.4	44.1	246
Ht (cm)	55	173	9.13	173	155	188
Body mass index (kg/m <sup>2</sup> )	55	31.2	10.6	30.4	16.5	77.9
Body surface area (m <sup>2</sup> )	55	2.11	0.38	2.08	1.42	3.57
Serum creatinine ( $S_{CR}$ ) (mg/dl)—all patients	55	2.20	2.42	1.19	0.3	13.1
$S_{CR}$ (mg/dl)—non-RRT patients	45	1.47	1.34	0.93	0.3	6.5
Albumin (g/liter)	55	2.29	0.62	2.40	1.0	3.6
Creatinine clearance ( $CL_{CR}$ ) (ml/min/1.73 m <sup>2</sup> )—all patients	55	104	61.4	97.8	12.5	380
$CL_{CR}$ (ml/min/1.73 m <sup>2</sup> )—non-RRT patients	45	102	63.2	86.5	21.2	380
Sex, male	30 (54.5)					
Race						
Caucasian	33 (60.0)					
Black or African American	21 (38.2)					
Other	1 (1.82)					
Ethnicity, non-Hispanic	54 (98.2)					
Diabetes	23 (41.8)					
Pulmonary hypertension	5 (9.09)					
Renal failure	18 (32.7)					
Heart failure	9 (16.4)					
Hepatic failure	6 (10.9)					
Receipt of vasopressors <sup>a</sup>	19 (34.5)					

<sup>a</sup>Received any one of the following within 24 h of start of infusion until 26 h after the start of infusion: norepinephrine, epinephrine, vasopressin, dopamine, phenylephrine, and dobutamine.

2 unbound plasma minocycline concentrations were below the lower limit of quantitation, these observations were excluded from the population PK analysis rather than implementing the likelihood-based Beal M3 method (13).

Summary statistics of baseline patient characteristics for the PK analysis population are presented in Table 1. The PK population was 54.5% male and 60.0% Caucasian. The mean (SD) age was 61.7 (15.1) years and ranged from 23 to 89 years, body weight was 93.3 (33.3) kg and ranged from 44.1 to 246 kg,  $CL_{CR}$  was 104 (61.4) ml/min/1.73 m<sup>2</sup> and ranged from 12.5 to 380 ml/min/1.73 m<sup>2</sup>, and albumin was 2.29 (0.618) g/liter and ranged from 1 to 3.6 g/liter. Four subjects had measured serum creatinine ( $S_{CR}$ ) less than 0.5 mg/dl, and for these individuals a capped value of 0.5 mg/dl was used in the computation of  $CL_{CR}$  to prevent derivation of nonphysiological  $CL_{CR}$  values. Of the 10 patients who received renal replacement therapy (RRT), 9 received intermittent hemodialysis (IHD) and 1 received continuous venovenous hemodialysis (CVVHD) at least once during the PK sampling period.

**Summary of total and unbound plasma minocycline concentrations.** The mean  $\pm$  SD of the observed total and unbound plasma minocycline concentration-time data are presented on a linear (Fig. 1A) and semilog (Fig. 1B) scale. Visual inspection of these plots indicated that both total and unbound minocycline concentrations declined in parallel and in a biphasic fashion following the end of the approximately 1-h i.v. infusion. A plot of the fraction of minocycline bound versus total minocycline concentration using time-matched data, including a focus on only those total minocycline concentrations less than 2 mg/liter, also demonstrated that the fraction unbound appeared to remain constant and independent of total minocycline concentration (Fig. 2).

**Population structural PK model selection.** During structural PK model development, several variations of the two-compartment model were evaluated (Table S1). The best structural PK model assumed that unbound minocycline concentrations were a constant fraction of the total minocycline concentrations, that both total and unbound minocycline concentrations could be cleared via IHD, and that no statistically significant

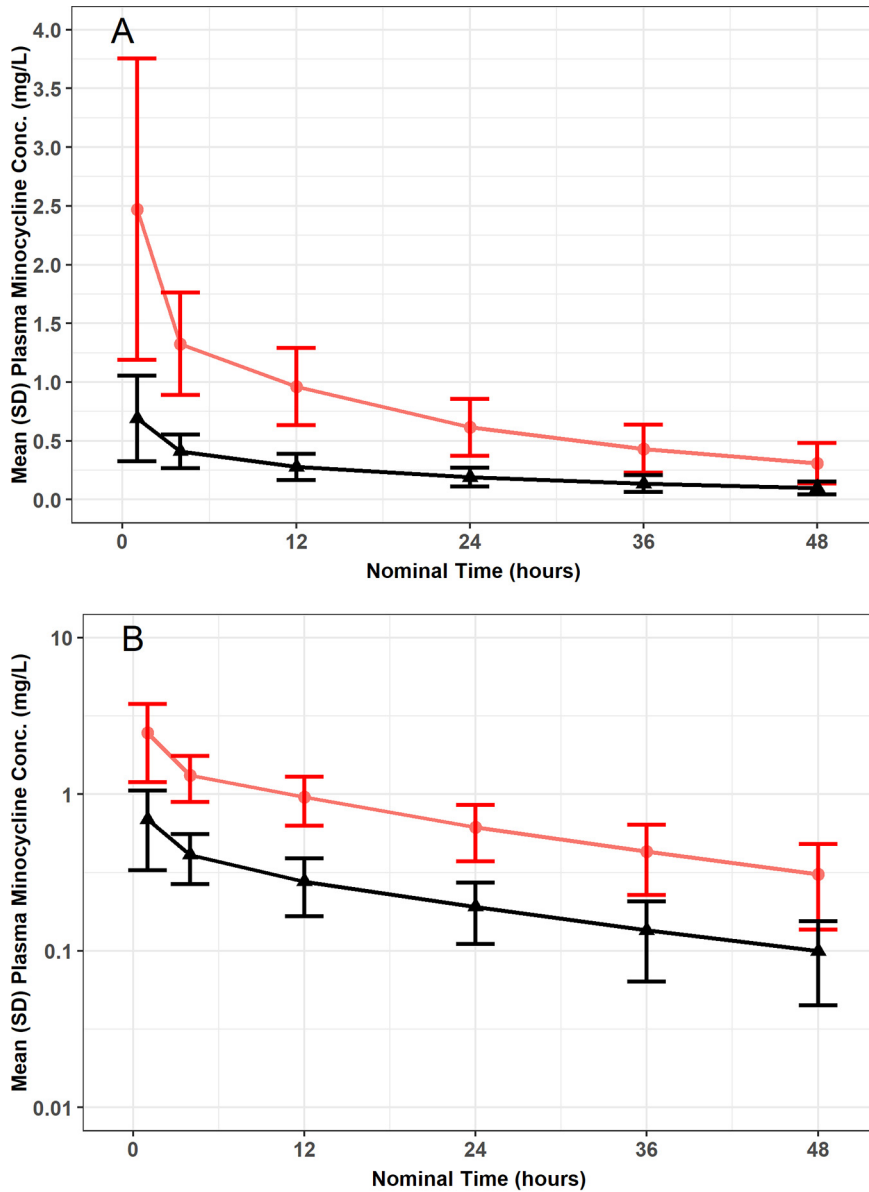


**FIG 1** Mean  $\pm$  SD of the observed total and unbound plasma minocycline concentration-time data following a single i.v. infusion of 200 mg minocycline over 1 h to critically ill patients, presented on a linear (A) and semilog (B) scale. Red lines are total minocycline concentrations, and black lines are unbound minocycline concentrations.

differences existed between venous PK samples and the small number of arterial PK samples ( $n = 12$ ) collected from three patients (including the one undergoing CVVHD). The final parameter estimates for this model are provided in Table 2. All structural PK model parameters were generally estimated with acceptable precision (standard error of the mean [SEM] of  $<50\%$ ), including the estimate of the  $CL_{IHD}$  parameter. The two-compartment model provided an unbiased and excellent fit overall to the data. Agreement between the observed and both the population predicted and individual *post hoc* predicted and total plasma minocycline concentrations was excellent ( $r^2 = 0.61$  and  $r^2 = 0.99$ , respectively). Similar agreement between the observed and both the population predicted and individual *post hoc* predicted unbound plasma minocycline concentrations was also seen ( $r^2 = 0.58$  and  $r^2 = 0.96$ , respectively).

**Final PK model selection after covariate analysis.** Plots of the individual *post hoc* parameter minus the population mean parameter versus patient covariates using the

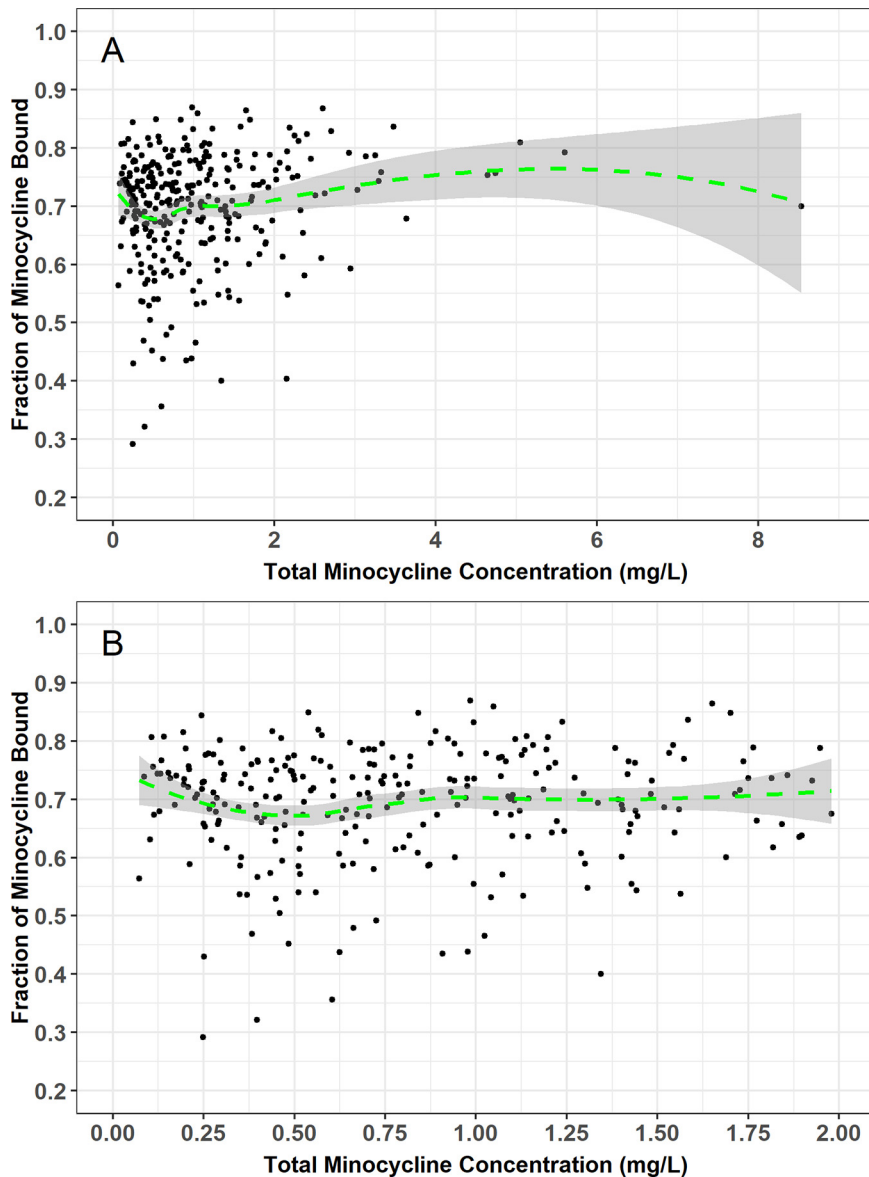


**FIG 2** Plot of fraction of minocycline bound versus total minocycline concentration using time-matched data from critically ill patients using all available data (A) and with focus on only those total minocycline concentrations less than 2 mg/liter (B). Green line and grey shaded region represent Loess smooth spline and 90% confidence interval.

base structural population PK model are provided in Appendix B in the supplemental material. Based upon this graphical screening procedure, only selected patient covariate-parameter relationships were formally tested within NONMEM as summarized in Appendix C in the supplemental material. In step 1 of forward selection of patient covariates, the effect of albumin on  $f_{ub}$ , when parameterized as a decreasing power function, was the most statistically significant parameter-covariate relationship ( $P = 0.00010$ ) and was added to form a new base structural PK model. This covariate effect reduced the magnitude of  $\omega^2$  for  $f_{ub}$  from 31.3% coefficient of variation (CV) to 27.0% CV. In step 2, the effect of body surface area (BSA) on central volume of distribution ( $V_c$ ), when parameterized as an increasing power function, was the most statistically significant parameter-covariate relationship ( $P = 0.00374$ ) and was added to the model. This covariate effect reduced the magnitude of  $\omega^2$  for  $V_c$  from 55.1% CV to 50.6% CV. No additional covariates were added to the model in step 3.

**TABLE 2** Parameter estimates and associated standard errors for the base and final two-compartment population PK model with constant fraction unbound<sup>a</sup>

Parameter	Base model		Final model <sup>b</sup>	
	Final estimate	%SEM	Final estimate	%SEM
CL (liters/h)	4.68	6.22	4.70	6.24
$V_c$ (liters) at median BSA of 2.08 m <sup>2</sup>	74.2	8.12	74.5	6.60
$V_c$ -BSA power			1.21	30.1
CL <sub>d</sub> (liters/h)	16.2	8.66	16.0	8.66
$V_p$ (liters)	58.6	5.81	58.9	5.89
$f_{ub}$ at median albumin of 2.40 g/dl	0.293	4.45	0.280	3.53
$f_{ub}$ -albumin power			-0.533	23.2
CL <sub>IHD</sub> (liters/h) <sup>c</sup>	5.57	46.7	5.55	46.8
$\omega^2$ for CL	0.209 (45.8% CV)	17.9	0.208 (45.6% CV)	18.1
$\omega^2$ for $V_c$	0.305 (55.2% CV)	31.0	0.250 (49.9% CV)	38.0
$\omega^2$ for $V_p$	0.111 (33.3% CV)	31.2	0.117 (34.1% CV)	30.7
$\omega^2$ for $f_{ub}$	0.0979 (31.3% CV)	32.3	0.0733 (27.1% CV)	35.4
Covariance ( $\eta_{CL}$ , $\eta_{Vc}$ )			0.101 ( $r^2 = 0.196$ )	34.5
Covariance ( $\eta_{fub}$ , $\eta_{Vp}$ )			0.0478 ( $r^2 = 0.266$ )	42.7
Residual variability ( $\sigma^2$ )				
Total minocycline	0.00832 (9.12% CV)	17.0	0.00843 (9.18% CV)	15.6
Unbound minocycline	0.0252 (15.9% CV)	18.3	0.0251 (15.8% CV)	17.6

<sup>a</sup>BSA, body surface area; CL, clearance;  $V_c$ , central volume of distribution; CL<sub>d</sub>, distribution clearance;  $V_p$ , peripheral volume of distribution;  $f_{ub}$ , fraction unbound; CL<sub>IHD</sub>, clearance related to active intermittent hemodialysis; SEM, standard error of the mean.

<sup>b</sup>Eta-shrinkage was  $\leq 3.16\%$  for CL,  $V_c$ , and  $f_{ub}$  while it was only 14.9% for  $V_p$ .

<sup>c</sup>Effective only during periods where intermittent hemodialysis was performed.  $\omega^2$  on CL<sub>d</sub> was negligible and fixed to zero in the model.

A scatterplot matrix of interindividual error terms (ETAs) indicated that the covariances between  $\eta_{CL}$  and  $\eta_{Vc}$ ,  $\eta_{fub}$  and  $\eta_{Vc}$ , and  $\eta_{fub}$  and  $\eta_{Vp}$  were the strongest and were considered part of the full multivariable PK model. The covariances between  $\eta_{CL}$  and  $\eta_{Vc}$  and between  $\eta_{fub}$  and  $\eta_{Vp}$  were successfully estimated in the full multivariable model and significantly reduced the NONMEM minimum value of the objective function (MVOF) (decrease of 20.187 with 2 df,  $P = 0.00004$ ). Covariance terms involving  $\eta_{Vc}$  were not included in the full multivariable model as they did not significantly lower the NONMEM MVOF and led to many covariance terms estimated with poor precision. Histograms of the ETAs for each structural PK model parameter were symmetrical and did not appear to deviate from normality.

During stepwise backward elimination, all of the covariate effects remaining in the model remained statistically significant at the more stringent  $\alpha = 0.001$ . The only exception was that the effect of BSA on  $V_c$  was marginally not statistically significant ( $P = 0.00145$ ), which is in part due to the small number of subjects in this study. However, this covariate effect was retained in the population PK model given the theoretical importance of body size in volume of distribution and the fact that the magnitude of  $\omega^2$  for  $V_c$  increased substantially when this covariate effect was removed.

The final parameter estimates for the final two-compartment population PK model are provided in Table 2. All population PK model parameters were estimated with acceptable precision (SEM < 50%), including the estimate of the CL<sub>IHD</sub> parameter. The population mean CL for total minocycline was estimated to be 4.70 liters/h, and the steady-state volume of distribution ( $V_c + V_p$ ) was 133 liters. The total minocycline CL<sub>IHD</sub> was estimated to be 5.55 liters/h, which was quantitatively similar to the total minocycline CL. The  $f_{ub}$  was estimated to be 0.280; the unbound minocycline CL was calculated to be 1.32 liters/h. The mean  $\pm$  SD half-lives at  $\alpha$  phase and  $\beta$  phase ( $T_{1/2,\alpha}$  and  $T_{1/2,\beta}$ , respectively) calculated using the individual *post hoc* parameters were  $1.36 \pm 0.456$  h and  $23.4 \pm 9.53$  h, respectively. The magnitude of  $\omega^2$  was 45.6% CV for CL, 49.9% CV for  $V_c$ , 34.1% CV for  $V_p$ , and 27.1% CV for  $f_{ub}$ . The residual variability was

**TABLE 3** Summary statistics of individual *post hoc* PK parameters and calculated exposures for total and unbound minocycline in ICU patients using the final two-compartment population PK model with constant fraction unbound for minocycline

Variable	<i>n</i>	Mean	SD	Median	Min	Max
Total $C_{max}$ (mg/liter)	55	2.58	1.33	2.24	0.539	7.88
Unbound $C_{max}$ (mg/liter)	55	0.749	0.364	0.629	0.238	2.21
$T_{max}$ (h)	55	1.02	0.0848	1.00	0.750	1.48
Total AUC <sub>0-24</sub> (mg · h/liter)	55	24.3	7.88	22.8	8.09	50.9
Total AUC <sub>0-∞</sub> (mg · h/liter)	55	46.6	19.7	44.4	15.1	96.7
Unbound AUC <sub>0-24</sub> (mg · h/liter)	55	7.18	2.46	7.12	2.74	13.3
Unbound AUC <sub>0-∞</sub> (mg · h/liter)	55	14.1	6.68	13.7	3.65	29.2
CL (liters/h)	55	5.24	2.63	4.50	2.07	13.2
$V_{ss}$ (liters)	55	146	57.0	140	54.7	465
$T_{1/2,\alpha}$ (h)	55	1.36	0.456	1.35	0.448	3.44
$T_{1/2,\beta}$ (h)	55	23.4	9.53	20.3	8.87	46.8
$f_{ub}$	55	0.309	0.120	0.280	0.159	0.957

9.18% CV and 15.8% for total and unbound minocycline, respectively. Summary statistics of individual *post hoc* PK parameters and calculated exposures for total and unbound minocycline in ICU patients using the final two-compartment population PK model are provided in Table 3.

The final two-compartment population PK model with constant  $f_{ub}$  provided an unbiased and excellent fit overall to the data (Fig. 3 and 4). Agreement between the observed and both the population predicted and individual *post hoc* predicted total ( $r^2 = 0.66$  and  $r^2 = 0.99$ , respectively) and unbound ( $r^2 = 0.67$  and  $r^2 = 0.96$ , respectively) plasma minocycline concentrations was excellent. Plots of the observed and individual *post hoc* predictions of total and unbound plasma minocycline for each patient further demonstrate the accuracy and precision of the PK model (Fig. S2); it can be seen that only one patient had comparable total and unbound minocycline concentrations, which could indicate assay error ( $f_{ub}$  was estimated to be  $>0.95$  for this patient). The addition of albumin and BSA as covariates on  $f_{ub}$  and  $V_{cr}$ , respectively, contributed to the improvement in the population mean predictions. Histograms of normalized prediction distribution errors (NPDE) for the fit of the final two-compartment population PK model (Fig. S3) were symmetrical around a mean value of zero and appeared to be normally distributed as would be expected if the fixed and random effects were specified correctly. Lastly, visual predictive checks for the fit of the final population model to the total and unbound plasma minocycline concentration-time data from ICU patients demonstrated excellent agreement between the median and 90% prediction interval of the observed and simulated unbound and total minocycline concentration-time data (Fig. 5), confirming the adequacy of the population PK model both for characterizing the existing data and for the purposes of performing simulations.

**Pharmacokinetic-pharmacodynamic target attainment assessment.** Results of the probability of free-drug plasma PK-PD target attainment analyses for i.v. minocycline 200 mg administered every 12 h (Q12H) under steady-state conditions are shown in Fig. 6. The probability of achieving the  $fAUC:MIC$  (free area under the curve above the MIC) target of 12 in plasma for net bacterial stasis was  $\geq 90\%$  of simulated patients for *A. baumannii* isolates with MIC values of  $\leq 1$  mg/liter. The probability of achieving the  $fAUC:MIC$  target of 18 in plasma for 1-log change in  $\log_{10}CFU$  was  $\geq 90\%$  of simulated patients for *A. baumannii* infections with MIC values of  $\leq 0.5$  mg/liter.

## DISCUSSION

This multicenter study was performed to evaluate the time course of both unbound and total plasma minocycline concentrations in critically ill patients using modern bioanalytical methods. Overall, the PK of i.v. minocycline in critically ill patients aligned with the data from PK studies in older healthy participants (6, 8, 11). Consistent with other tetracyclines, a two-compartment population PK model with zero-order i.v. input

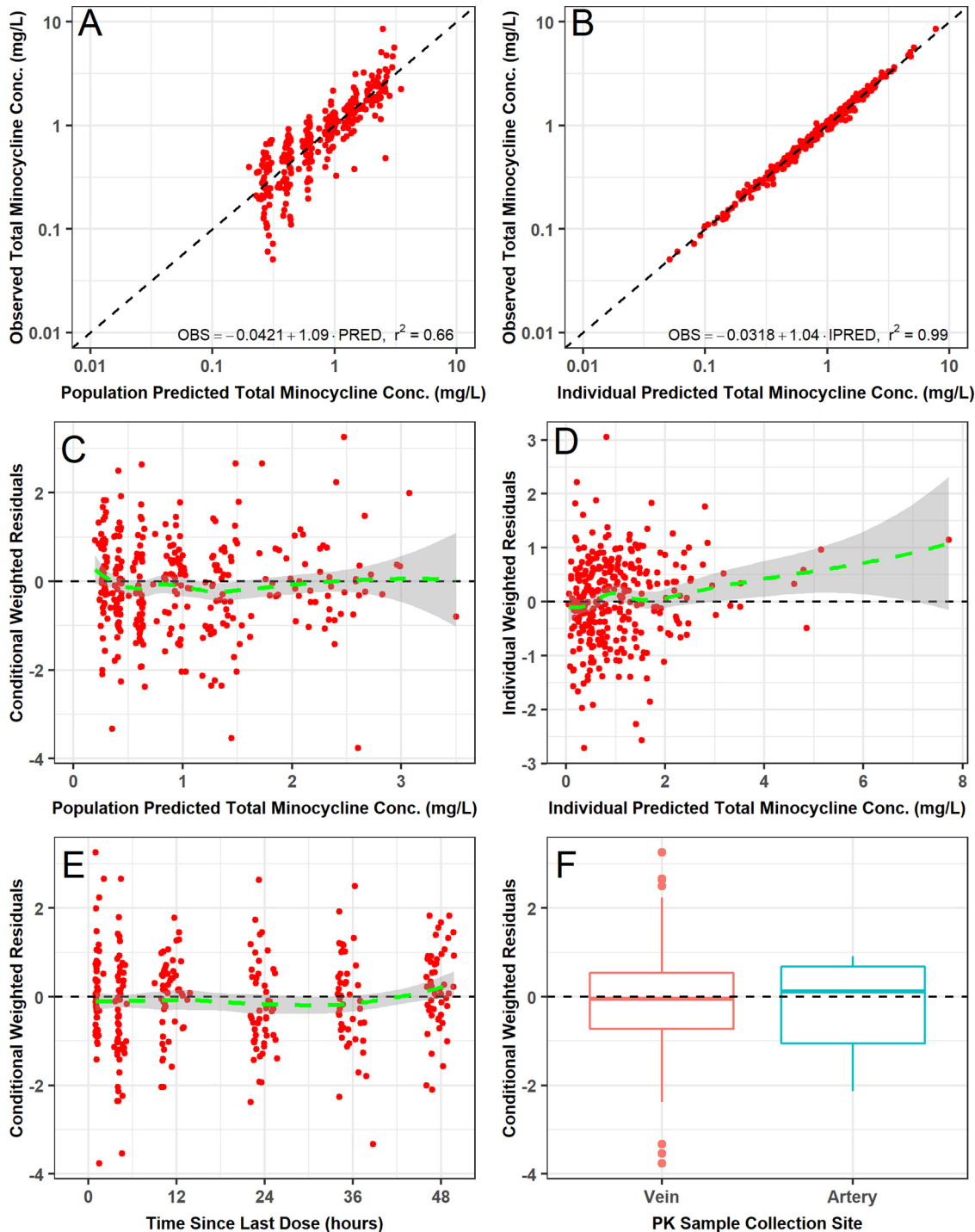


**FIG 3** Goodness-of-fit plots for the fit of the final two-compartment population PK model with constant fraction unbound to the total plasma minocycline concentration-time data from critically ill patients.

and first-order elimination with a constant  $f_{ub}$  best characterized the total plasma minocycline concentration-time data from critically ill patients (14). The median of the individual *post hoc*  $T_{1/2,\beta}$  values from these critically ill patients was 20.3 h and fell within the previously reported range of elimination half-life values of 15 to 23 h (6, 8, 11, 15). The median volume of distribution at steady state ( $V_{ss}$ ) and CL observed in ACUMIN were slightly higher than previous reports, but this was likely a function of the greater variability around PK exposure estimates (e.g.,  $V_{ss}$  and CL) in critically ill patients

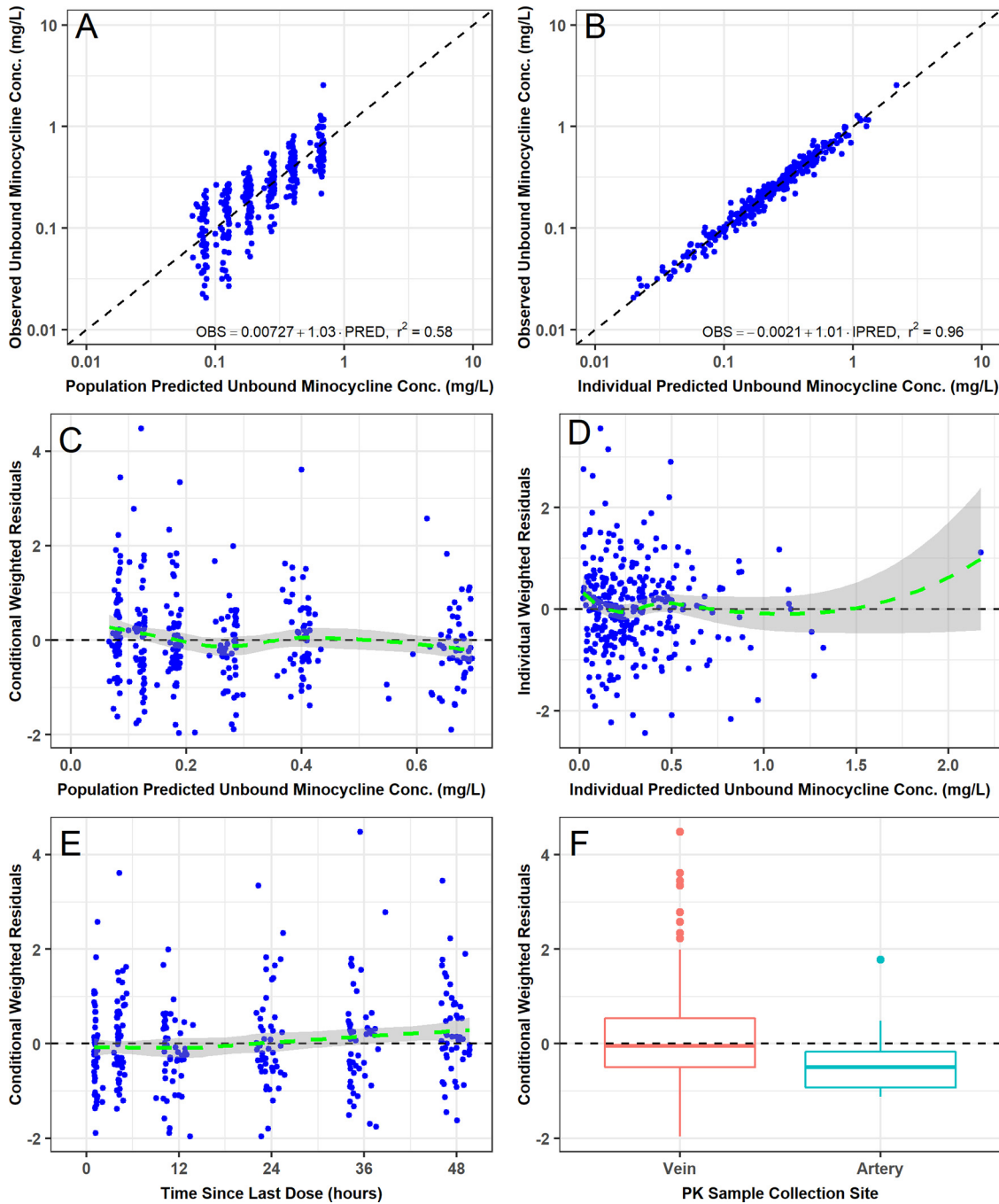


**FIG 4** Goodness-of-fit plots for the fit of the final two-compartment population PK model with constant fraction unbound to the unbound plasma minocycline concentration-time data from critically ill patients.

relative to studies of healthy participants, and this speaks directly to the differing physiological states across patients in the ICU.

The findings do not support the current paradigm that tetracyclines exhibit inverse nonlinear protein binding across the range of minocycline concentrations observed in this study (0.05 to ~4 mg/liter as shown in Fig. 2) (16), which had been proposed based on protein binding estimates derived from *in vitro* and animal studies (17). A distinguishing feature of this study was the determination of both total and unbound minocycline concentrations at each PK collection time point. The ability to comodel both unbound and total minocycline concentrations allows for direct estimation of the

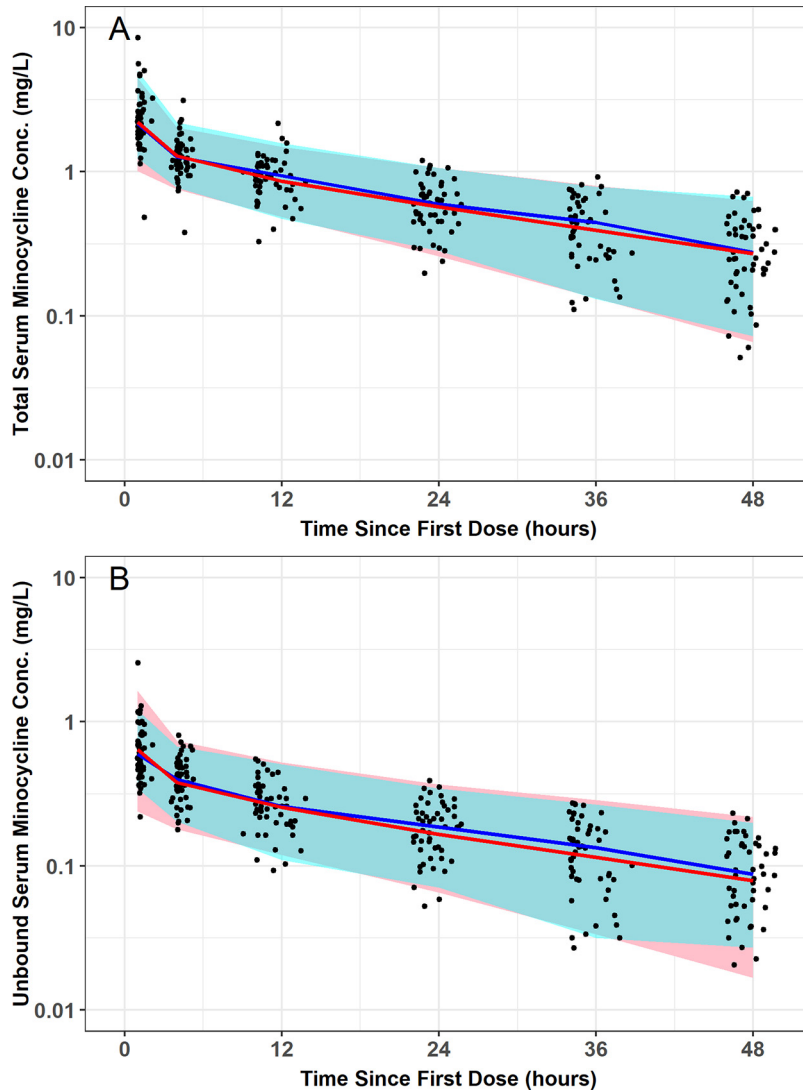


**FIG 5** Visual predictive check for the fit of the final two-compartment population PK model with constant fraction unbound to the total and unbound plasma minocycline concentration-time data from critically ill patients. Red (simulated) and blue (observed) indicate median and 90% prediction interval; black dots are observed data.

fraction of unbound drug at any given time and for evaluation of whether this fraction was constant or a function of total minocycline concentration. In the current analysis, a two-compartment population PK model with an estimated constant  $f_{ub}$  for minocycline enabled simultaneous characterization of the time-matched total and unbound plasma minocycline concentration-time data collected in this study. Other structural models with nonlinear protein binding were considered but none improved model fit (see Table S1 in the supplemental material). Selection of a two-compartment population PK model with an estimated constant  $f_{ub}$  is further supported by a plot of the bound versus total minocycline concentrations using the observed time-matched PK data, which clearly demonstrate that  $f_{ub}$  is independent of the total minocycline concentration. Finally, the total and unbound minocycline concentration-time curves within each patient are parallel to each other, supporting that  $f_{ub}$  is constant and not related to the observed total concentration.

The finding that  $f_{ub}$  for minocycline was constant is consistent with the current understanding of the rapid equilibrium assumption between protein-bound and unbound drug (18–20). In short, the protein-bound fraction of drug appears to act as a

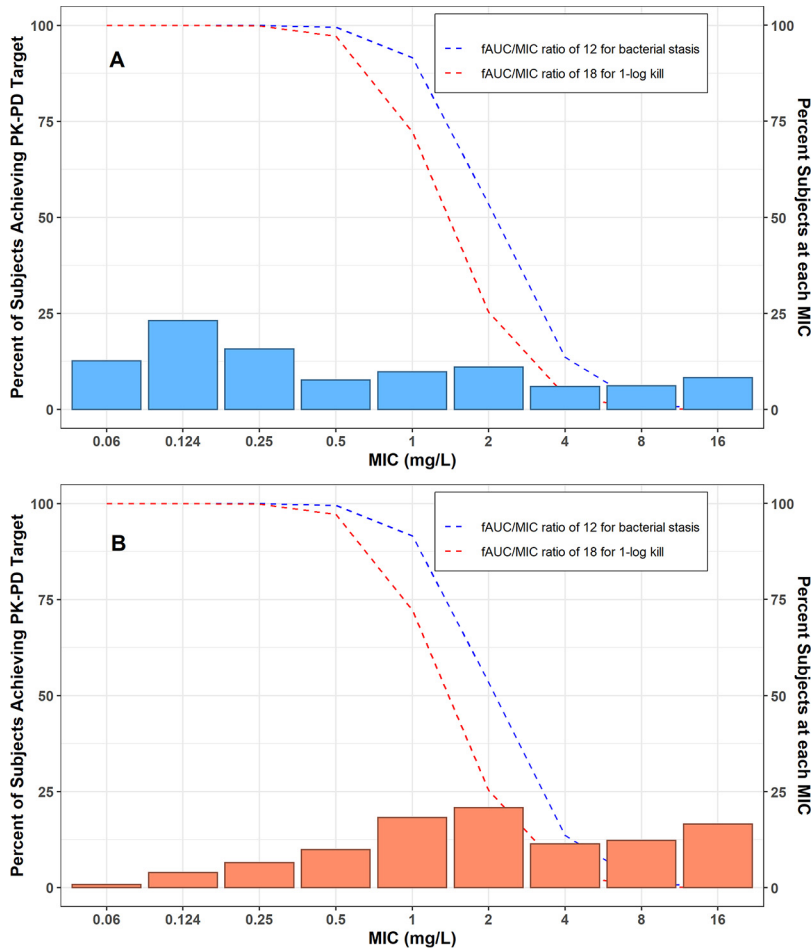


**FIG 6** Percentage of simulated patients achieving the *f*AUC:MIC plasma targets of either 12 (net bacterial stasis) or 18 (1- $\log_{10}$ CFU kill) for the 200 mg i.v. Q12H minocycline dosing regimen at steady state conditions against (A) *A. baumannii-A. calcoaceticus* complex and (B) multidrug resistant (MDR) *A. baumannii-A. calcoaceticus* complex (7).

reservoir within the central compartment as it is expected that only unbound drug is distributed to tissues and/or eliminated from the body. As unbound drug distributes to tissues and/or is eliminated from the body, bound drug rapidly dissociates from albumin and other circulating proteins. This rapid dissociation preserves the equilibration between bound and unbound drug and results in proportional distribution and clearance terms between the bound and unbound fraction of drugs. If rapid equilibration did not occur, the PK profiles for total and unbound minocycline concentrations in plasma would not have declined in parallel, as was observed in this study, and PK models with nonlinear protein binding would have fit our data more closely.

The findings also demonstrate a lack of association between CL and  $CL_{CR}$ . This finding was not surprising given that  $CL_{CR}$  was found to contribute only <11% to the total CL in previous studies of subjects with normal renal function in which urinary excretion of minocycline was measured (6, 11). However, this finding is clinically important, confirming no need for minocycline dosage adjustments in patients with renal impairment. Although patients on RRT were included in the study population, this study was not designed to evaluate the impact of RRT on the PK of minocycline. Consistent with other PK studies in critically ill patients that include patients on RRT (39), our methodology determined if plasma clearance was augmented in patients on IHD. The minocycline concentrations observed in IHD patients indicates that there was some increased clearance during the times that IHD was administered.

The two covariates retained in the final population PK model (BSA associated with

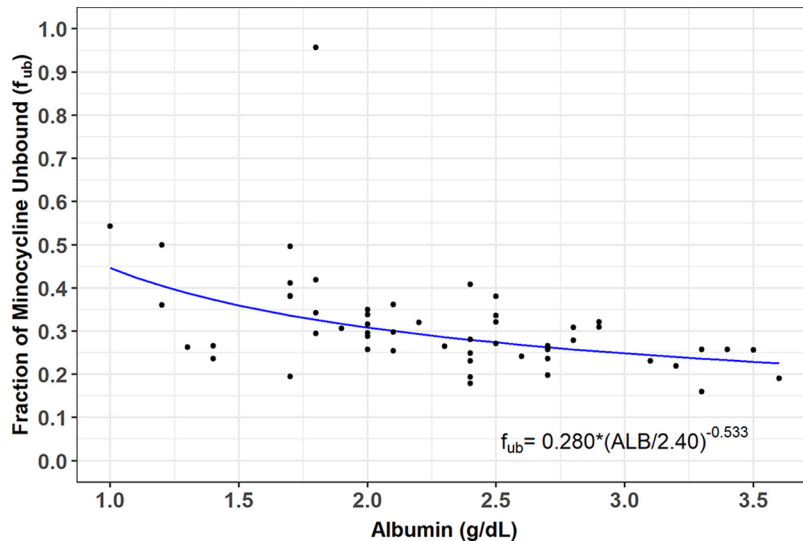


**FIG 7** Model-predicted typical value of the fraction of minocycline bound ( $f_{ub}$ ) versus albumin concentration, overlaid upon the individual *post hoc*  $f_{ub}$  values obtained using the final population PK model characterizing the total and unbound plasma minocycline concentration-time data from critically ill patients.

$V_c$  and albumin associated with  $f_{ub}$ ) were not unexpected and are biologically plausible. The volume of distribution of many drugs increases with body size, and circulating plasma proteins like albumin can directly contribute to reducing the free fraction of many drugs. While studies suggest that systemic exposures are reduced in patients with hypoalbuminemia due to increases in  $V_{ss}$  and CL secondary to increased  $f_{ub}$  (21), we did not find this to be the case for minocycline, as CL was found to be independent of albumin.

We do not anticipate that BSA differences across critically ill patients will have any bearing on achieving critical PK-PD targets since changes in  $V_c$  do not affect the AUC. However, the association between  $f_{ub}$  and albumin may have implications for clinical practice for critically ill patients as the extent of unbound drug is driven, in part, by  $f_{ub}$ . The observed albumin concentrations in the ACUMIN study ranged from 1.0 to 3.6 g/dl (normal range for albumin in healthy subjects is typically 3.4 to 5.4 g/dl). The model predicted  $f_{ub}$  varying from 0.446 to 0.236 over the range of 1 g/dl to 3.4 g/dl (Fig. 7). Although  $f_{ub}$  appears to flatten at higher albumin concentrations, the model predicts that  $f_{ub}$  would decrease to 0.182 for patients with albumin levels at the upper range of normal (5.4 g/dl). Of note, the model-predicted range of  $f_{ub}$  for subjects with normal albumin concentrations (0.182 to 0.236) would be qualitatively similar to values previously reported for minocycline of 24% (11). Given the predicted increase in  $f_{ub}$  over the albumin range of 1 g/dl to 3.6 g/dl, the probability of PK-PD target attainment profile may be less robust among individuals with albumin levels in the normal range than among those with extremely low albumin concentrations. However, the model predicts that a doubling in the  $f_{ub}$  will shift the probability of target attainment profile downward, at most, by only  $\sim 1$  MIC doubling dilution, assuming there are no corresponding changes in CL (21).

It is important to note that the low albumin levels observed in ACUMIN do not mitigate the external generalizability of the findings. Hypoalbuminemia is commonplace in critically ill patients, with reported incidences as high as 40 to 50% (22). However, the findings from ACUMIN should be applied only to critically ill patients with similarly low albumin concentrations. Studies suggest that systemic exposures are reduced in patients with hypoalbuminemia due to increases in  $V_{ss}$  and CL secondary to increased  $f_{ub}$  (21). Although we did observe an association between CL and albumin, the extent of protein binding observed in the ACUMIN study population may have contributed to the faster CL values reported in this study relative to historical values.

Further PK data are needed to clarify the effect of albumin on  $f_{ub}$  for minocycline in patients with normal albumin, and extrapolation of our findings to patients with normal albumin concentrations should be done with caution.

Lastly, the findings from the probability of  $fAUC:MIC$  in plasma target attainment analyses suggest that the current i.v. minocycline dosing employed in clinical practice confers a suboptimal (<90%) probability of microbiologic efficacy in plasma for a proportion of critically ill patients with *A. baumannii* infections. Minocycline 200 mg i.v. Q12H, the maximum daily dosing regimen recommended in the product labeling, only achieved the critical  $fAUC:MIC$  targets in plasma associated with stasis and  $-1$ -log killing for *A. baumannii* isolates with MIC values of  $\leq 1$  mg/liter. In a recent U.S. surveillance MIC study consisting of 1,081 clinical isolates of *A. baumannii*-*A. calcoacet*-*ticus* complex by Flamm et al. (7), 31.3% of isolates had a MIC value of  $>1$  mg/liter. Among MDR *A. baumannii*-*A. calcoacet*-*ticus* complex, the minocycline MIC value was  $>1$  mg/liter for 60% of the tested isolates (Fig. 6). Assuming  $f_{ub}$  remains constant at concentrations higher than that observed in this study, a 1,600-mg i.v. Q12H minocycline dosing regimen would be required to ensure  $>90\%$  probability of achieving the  $fAUC:MIC$  target associated with stasis in plasma for *A. baumannii* isolates up to the  $MIC_{90}$  (e.g., MIC of  $\leq 8$  mg/liter) that was observed in the surveillance study by Flamm and colleagues (7). As  $f_{ub}$  may not remain constant at concentrations higher than that observed in our study, our simulation result of the 1,600 mg i.v. Q12H dosing regimen should be interpreted with caution. While i.v. minocycline daily doses of  $\geq 400$  mg appear safe in acute stroke/actual spinal cord injury patients (23, 24), little to no information exists with daily doses of i.v. minocycline in excess of 400 mg in critically ill patients with infections. In a recent phase 1 study of healthy adult subjects, single i.v. doses of minocycline up to 600 mg were well tolerated, and the maximum tolerated multidose was 300 mg i.v. twice daily (40). Thus, higher i.v. minocycline daily doses like those used in acute stroke/actual spinal cord injury patients and healthy subjects cannot be endorsed at this time in critically ill patients with infections. Use of higher i.v. minocycline doses in critically ill patients with infections requires a detailed risk-versus-benefit assessment as many of the toxicities associated with minocycline, like azotemia, hyperphosphatemia, acidosis, and other metabolic disturbances, are related to the extent of systemic exposure (8).

Like all studies of this nature, a certain degree of caution should be exercised in interpreting the findings from the probability of  $fAUC:MIC$  plasma target attainment analyses. The  $fAUC:MIC$  targets in plasma utilized were derived from a preclinical PK-PD infection model (12), and no clinical exposure-response studies are available to judge the adequacy of current dosing. Preclinical PK-PD infection model studies are an integral part of the drug development process and are used to inform dose and schedule selection, especially for the treatment of highly resistant bacterial pathogens when limited clinical data are available to define optimal therapy (25–27). Furthermore, the plasma PK-PD targets utilized were obtained from an immunocompetent rat pneumonia infection model of *A. baumannii* and, accordingly, likely reflect the  $fAUC:MIC$  targets in plasma required for bacterial killing in the lung (12). It is well established that minocycline achieves greater concentrations in the lungs than in plasma (28, 29). Although the concentrations of minocycline were not assayed in the epithelial lining fluid (ELF) in the immunocompetent rat pneumonia infection model of *A. baumannii* study, it is reasonable to surmise that these  $fAUC:MIC$  plasma targets are reflective of the higher concentrations achieved in the ELF (i.e., site of infection) that are needed for bacterial killing in the lung. Based on the probability of achieving the  $fAUC:MIC$  plasma targets derived in an immunocompetent rat pneumonia infection model of *A. baumannii*, combination antibiotic therapy should be potentially considered in patients with *Acinetobacter* sp. infections, especially MDR strains. Given that the probability of attainment analyses were based on  $fAUC:MIC$  plasma targets from an animal model, there is also the need for clinical validation (30).

In summary, a two-compartment population PK model with zero-order i.v. input and first-order elimination, with an estimated constant  $f_{ub}$ , best characterized the total and

unbound plasma minocycline concentration-time data in critically ill patients. In the  $fAUC:MIC$  plasma target attainment analyses using the final population PK model, the 200-mg i.v. Q12H minocycline dosing regimen currently employed in clinical practice was predicted to result in a suboptimal  $fAUC:MIC$  profile in plasma for nearly a third of patients with *A. baumannii* infections, and daily doses of  $\geq 400$  mg a day would be needed to adequately cover *A. baumannii* infections with MIC values of  $>1$  mg/liter. Although i.v. minocycline was found to be safe in this single i.v. dose PK study in critically ill patients, clinicians need to conduct a detailed risk-versus-benefit assessment when contemplating the use of higher minocycline doses for their patients. Like all PK-PD profiling studies of this nature, these findings need clinical confirmation. Clinicians should potentially consider using combination antibiotic therapy when using i.v. minocycline in patients with *Acinetobacter* sp. infections, especially those caused by MDR strains, based on the findings from the probability of target attainment analyses. The findings from the study also suggest that the current minocycline FDA susceptibility breakpoint of  $\leq 4$  mg/liter should perhaps be revisited in future clinical investigations to validate the probability of target analyses, which were based on  $fAUC:MIC$  plasma targets derived in a rat pneumonia model of *A. baumannii*.

## MATERIALS AND METHODS

**Study design and treatment administration.** The ACUMIN Study (ClinicalTrials.gov identifier NCT03369951) was a phase IV, multicenter, open-label multicenter study to evaluate the PK of a single dose of i.v. minocycline in up to 50 evaluable, ICU patients already receiving antimicrobial therapy for a known or suspected Gram-negative infection (31). Study criteria and the definition of the PK evaluable population are listed in Appendix A in the supplemental material. Institutional review board approval was obtained at each participating center. Once patients were confirmed as eligible, and informed consent was obtained, patients were enrolled into the study. Each subject received a single 200 mg i.v. infusion of minocycline in 100 ml of normal saline administered at a rate of 100 ml/h until the bag was empty and the line was flushed. Safety assessments performed are included in Appendix A in the supplemental material.

**Pharmacokinetic sample collection.** Blood samples (6 ml) to assess the PK of minocycline were collected over a 48-h period after treatment administration, preferably from the arm contralateral to the one used for i.v. infusion. Blood samples were collected predose, immediately after infusion termination ( $\sim 1$  h), and at 4, 12, 24, 36, and 48 h after treatment administration. For each PK blood sample, plasma was separated into 2 aliquots. One plasma aliquot was used for determination of total minocycline. For the other plasma aliquot, centrifugation was used to generate ultrafiltered plasma for determination of unbound minocycline. Both aliquots were stored frozen until being shipped to the central laboratory for testing. Methods for the determination of minocycline in human EDTA K2 plasma were validated at the Syneos Health bioanalytical lab (Quebec, Canada). The total plasma PK samples were used to analyze total minocycline concentrations, and the ultrafiltered plasma was used to determine unbound minocycline. Plasma PK samples were analyzed for both unbound and total minocycline concentrations using liquid chromatography-tandem mass spectrometry (LC-MS/MS) (AB Sciex API 5000 equipped with an electrospray).

**LC-MS/MS methods for the determination of total minocycline.** The samples with minocycline and the internal standard (IS) (Minocycline-d6) are cleaned by liquid-liquid extraction using ethyl acetate. After vortex and centrifugation, 50  $\mu$ l of the organic phase is transferred by the liquid handling system in a 96-well plate. Samples are then evaporated and reconstituted with 200  $\mu$ l of a methanol-water solution. A 15- $\mu$ l sample is injected into the LC-MS/MS system for analysis. The LC-MS/MS analyses were carried out with an AB Sciex API 5000 equipped with a turbo ion spray source operated in the positive ionization mode. Chromatographic separation was carried out on a Life Sciences Ace 3-C<sub>18</sub> column (50 mm by 4.6 mm, 3  $\mu$ m). The MS operating conditions were optimized as follows. The ion spray voltage was set at 4,000, and the source temperature was maintained at 500°C. The collision energy was set at 25. Quantification was obtained by using multiple reaction monitoring (MRM) mode of the transitions at  $m/z$  458.4  $\rightarrow$  441.2 for minocycline and at  $m/z$  464.3  $\rightarrow$  447.1 for IS, respectively. Data acquisition and integration of multiple reaction monitoring chromatograms were performed using the software package Analyst 1.6.3. (AB Sciex, Toronto, Canada). A linear regression (weighted  $1/\times 2$ ) was applied to a plot of the peak area ratio versus concentration for the standards to obtain the calibration curve. The standard curve range is 40 to 10,000 ng/ml. Interassay precision for quality controls (QCs) was as follows: biases,  $-4.85$  to  $0.39\%$ ; CV, 2.61 to 5.84%.

**LC-MS/MS methods for the determination of unbound minocycline.** The samples with unbound minocycline and the internal standard (Minocycline-d6) are cleaned by liquid-liquid extraction using ethyl acetate. After vortexing and centrifugation, 100  $\mu$ l of the organic phase is transferred by the liquid handling system in a 96-well plate. Samples are then evaporated and reconstituted with 200  $\mu$ l of a methanol-water solution. A 15- $\mu$ l sample is injected into the LC-MS/MS system for analysis. The LC-MS/MS analyses were carried out with an AB Sciex API 5000 equipped with a turbo ion spray source operated in the positive ionization mode. Chromatographic separation was carried out on a Life Sciences Ace 3-C<sub>18</sub> column (50 mm by 4.6 mm, 3  $\mu$ m). The MS operating conditions were optimized as follows. The

ion spray voltage was set at 4,000, and the source temperature was maintained at 500°C. The collision energy was set at 31. Quantification was obtained by using multiple reaction monitoring (MRM) mode of the transitions at  $m/z$  458.3  $\rightarrow$  441.0 for minocycline and at  $m/z$  464.2  $\rightarrow$  447.1 for IS, respectively. Data acquisition and integration of multiple reaction monitoring chromatograms were performed using the software package Analyst 1.6.3. (AB Sciex, Toronto, Canada). A linear regression (weighted  $1/\times 2$ ) was applied to a plot of the peak area ratio versus concentration for the standards to obtain the calibration curve. The standard curve range is 20 to 3,000 ng/ml. Interassay precision for QCs was as follows: biases,  $-6.68$  to  $-0.26\%$ ; CV, 3.22 to 5.38%.

**Population PK analysis. (i) Structural PK model selection.** The population PK analysis was conducted using NONMEM version 7.3 (Icon Development Solutions, Ellicott City, MD) implementing the first-order conditional estimation method with  $\eta$ - $\varepsilon$  interaction (FOCEI). Based on prior minocycline PK modeling studies (11), a two-compartment model with zero-order input and first-order elimination to simultaneously fit the total and unbound plasma minocycline concentration-time data was used as the structural PK model. The two-compartment model was parameterized using total clearance (CL, in liters/h), central volume of distribution ( $V_c$ , in liters), distribution clearance between the central and peripheral compartment (CL<sub>d</sub>, in liters/h), and the volume of distribution for the peripheral compartment ( $V_p$ , in liters). An additional CL term (CL<sub>IHD</sub>) was included to account for total minocycline removed during periods of intermittent hemodialysis (IHD). Based upon exploratory graphical analyses of the total and free minocycline concentration-time profiles, the fraction of minocycline unbound ( $f_{ub}$ ) was assumed to remain as a constant function of total minocycline concentration in order to comodel the unbound and total minocycline concentration-time data. Unbound minocycline concentrations at any given time were determined as the product of total minocycline concentrations and  $f_{ub}$ . Interindividual variability ( $\omega^2$ ) was estimated for CL,  $V_c$ , CL<sub>d</sub>,  $V_p$ , and  $f_{ub}$  using exponential error models. Separate combined additive plus constant coefficient of variation (CCV) error models were used to describe residual variability ( $\sigma^2$ ) for the unbound and total plasma minocycline concentrations.

Other structural PK models or modifications, such as inclusion of nonlinear plasma protein binding as a function of total minocycline concentration (16, 17), were also considered to identify the most parsimonious model which provided the best possible fit to the data. Saturable protein binding was implemented using a quasiequilibrium binding model, similar in nature to a target-mediated drug disposition model, in which the maximal binding capacity ( $B_{max}$ , in milligrams/liter) and binding dissociation constant ( $K_D$ , in milligrams/liter) were estimated (32, 33). Using this approach, the  $f_{ub}$  would not be constant and free minocycline concentrations would instead be a nonlinear function of the total minocycline concentrations.

Population PK models were assessed by evaluating the individual and population mean PK parameter estimates for minocycline, and their precision as measured by the percent standard error of the population mean estimate (%SEM), along with the ability to reduce the magnitude of the unexplained  $\sigma^2$  and  $\omega^2$ . Graphical examination of standard diagnostic and population analysis goodness-of-fit plots was also considered, such as observed versus both population and individual *post hoc* predicted total and unbound minocycline concentrations; conditional population weighted residuals versus time since last dose, population predicted total and unbound minocycline concentrations, and potentially other independent variables; individual weighted residuals versus individual *post hoc* predicted total and unbound minocycline concentrations; and the agreement between the observed and individual *post hoc* predicted plasma minocycline concentration-time data (individual observed and predicted overlays). Lastly, a likelihood ratio test was used to assess the statistical significance of adding or deleting a parameter from the model based upon differences in minimum value of the objective function (MVOF) for nested models, and Akaike's information criterion (AIC) was used to compare nonnested models (34).

**(ii) Final PK model selection after covariate analysis.** After developing a base structural population PK model to describe the unbound and total plasma minocycline concentrations, a formal covariate analysis was performed using stepwise forward selection ( $\alpha = 0.01$ ) and backward elimination ( $\alpha = 0.001$ ) techniques as described in detail in Appendix A in the supplemental material. Patient demographic descriptors considered in the covariate analysis included sex, age in years, weight in kilograms, height in centimeters, body surface area (BSA) in square meters (35), body mass index (BMI) in kilograms/square meter, and ideal body weight (IBW) in kilograms. Clinical laboratory data utilized as covariates included serum creatinine ( $S_{CR}$ ) in milligrams/deciliter, albumin in grams/deciliter, and calculated CL<sub>CR</sub> in milliliters/minute/1.73 m<sup>2</sup> using the Cockcroft and Gault method and normalized to a BSA of 1.73 m<sup>2</sup> (36–38). Other disease-related indices such as the presence of diabetes, hepatic cirrhosis, pulmonary hypertension, organ transplantation, renal failure, and lastly heart failure as well as the corresponding New York Heart Association (NYHA) class were evaluated as patient covariates. Information pertaining to receipt of any renal replacement therapy (RRT) were collected from 1 h after start of infusion through 48 h after start of infusion. The approach used to account for RRT in the population PK model was determined based upon the type of RRT utilized, the timing and duration of RRT relative to dosing and PK sample collection, and potentially other more detailed information provided for each patient. For patients on continuous RRT, the effluent dialysis rate was substituted for CL<sub>CR</sub> during covariate evaluation.

The final population PK model after covariate analyses was assessed using the same model diagnostic and evaluation criteria as described previously. Covariances between the interindividual variability (IIV) terms were evaluated and estimated in the variance-covariance matrix for the final population PK model if warranted. In addition, the overall distribution of the normalized prediction distribution errors (NPDE) provided by NONMEM for the unbound and total plasma minocycline concentrations was evaluated and

compared to a normal distribution to determine if the fixed or random effects models were biased. The final population PK model was further evaluated and qualified by performing a visual predictive check (VPC), which graphically examined the agreement between the 5th, 50th, and 95th percentiles of the observed and the individual simulated unbound and total plasma minocycline concentrations across time intervals.

**(iii) Generation of individual pharmacokinetic parameters.** The individual patient dosing histories were utilized along with the individual *post hoc* PK parameters to generate unbound and total plasma minocycline concentration-time profiles and calculate unbound and total plasma minocycline exposure measures (maximum concentration of drug in plasma [ $C_{max}$ ],  $AUC_{0-24}$  and  $AUC_{0-\infty}$ ). The  $C_{max}$  was calculated for each simulated patient as the maximum simulated concentration. The  $AUC_{0-24}$  was calculated using numerical integration using the data from 0 to 24 h postdose. The  $AUC_{0-\infty}$  was calculated as dose/CL. The steady-state volume of distribution ( $V_{ss} = V_c + V_p$ ), alpha-phase half-life ( $T_{1/2,\alpha}$ ), and beta-phase half-life ( $T_{1/2,\beta}$ ) were calculated using the individual *post hoc* PK parameters.

**(iv) Pharmacokinetic-pharmacodynamic target attainment assessment.** Using the final population PK model including all statistically significant covariate effects, Monte Carlo simulation was performed using R (via the MRGSOLVE package). Simulated total and unbound minocycline concentrations for 2,000 virtual patients (non-IHD patients) were generated at steady state for the FDA-approved i.v. minocycline dosing regimen of 200 mg administered every 12 h. Virtual patients were simulated from normal distributions using the same mean (SD) BSA of 2.11 (0.38) and albumin of 2.29 (0.62) as was observed in the ACUMIN study population. The percentage of simulated patients achieving an *fAUC*:MIC target of either 12 or 18 during the 12-h dosing interval at steady-state was assessed over a range of MIC values observed for *A. baumannii*. These free PK-PD targets in plasma were based on the results of a rat lung pneumonia infection model, which demonstrated that bacterial stasis and 1-log change in  $\log_{10}$ CFU in the lungs with minocycline against four different clinical isolates of *A. baumannii* (MICs ranged from 0.25 to 4 mg/liter) were achieved at *fAUC*:MIC ratios in plasma of 12 and 18, respectively (12). Recent surveillance MIC data for *A. baumannii*-*A. calcoaceticus* complex and MDR *baumannii*-*A. calcoaceticus* complex published by Flamm et al. were utilized in the PK-PD target attainment analysis (7).

## SUPPLEMENTAL MATERIAL

Supplemental material is available online only.

**SUPPLEMENTAL FILE 1**, PDF file, 2.2 MB.

## ACKNOWLEDGMENTS

Research reported here was supported by the National Institute of Allergy and Infectious Diseases of the National Institutes of Health under award number UM1AI104681. The content is solely the responsibility of the authors and does not necessarily represent the official views of the National Institutes of Health. Vance Fowler, Jr., was supported by midcareer mentoring award K24-AI093969 from the NIH.

We thank Michael Dudley, David Griffith, and Jeffery Loutit for this assistance with the concept and design of the study. We thank Melinta Therapeutics for providing scientific input and supplying minocycline for this study. We would also like to thank Kenan Gu for his critical review of the manuscript.

T.P.L. is a consultant for Melinta. R.G.W. is a consultant for Melinta. F.P.S. received research funding from Ansun, Shire, Novartis, and Gilead. M.D.S. is a principal investigator of clinical trials from Curetis GmbH, Shire, Epigenomics Inc., Genentech Inc., Finch Therapeutics, Seres Therapeutics Inc., Janssen Research and Development LLC, Merck and Co., Diasorin Molecular, Prenosis, Summit Therapeutics, Leonard-Meron Biosciences, Kinevant Sciences, and Regeneron. V.F. reports personal fees from Novartis, Novadigm, Durata, Debiopharm, Genentech, Achaogen, Affinium, Medicines Co., Cerexa, Tetrphase, Trius, MedImmune, Bayer, Theravance, Basilea, Affinergy, Janssen, xBiotech, Contrafact, Regeneron, Basilea, Destiny, Amphliph Biosciences, Integrated Biotherapeutics; C3J, grants from NIH, MedImmune, Cerexa/Forest/Actavis/Allergan, Pfizer, Advanced Liquid Logics, Theravance, Novartis, Cubist/Merck; Medical Biosurfaces; Locus; Affinergy; Contrafact; Karius; Genentech, Regeneron, Basilea, Janssen, from Green Cross, Cubist, Cerexa, Durata, Theravance; Debiopharm, royalties from UpToDate; a patent sepsis diagnostics pending; and stock options for Valanbio. A.K. reports grants from United Therapeutics, grants from Actelion Pharmaceuticals, grants from Regeneron, grants from Cheetah Medical, and grants from Reata Pharmaceuticals, outside the submitted work. S.V.W. owns Enhanced Pharmacodynamics LLC, which served as a contractor for Emmes Corporation on this submitted work and also consults for over 80 biotech and pharmaceutical companies as well as various NIH investigators. All other authors have no disclosures to report.

Researchers interested in accessing the clinical trial data presented here are encouraged to submit a research proposal and publication plan. The proposal and plan will be reviewed by the ARLG publications committee and/or appropriate study team members. If approved and upon receipt and approval of a signed data access/use agreement, individual participant data necessary to complete the proposed analysis will be made available. Related documents, including the study protocol, statistical analysis plan, and data dictionary, may also be shared. Access to data will be granted only to researchers who provide a methodologically and scientifically sound proposal. Proposed analyses that are duplicative of ongoing or proposed analyses may not be supported. To submit a proposal, please complete a proposal at <https://arlg.org/how-to-apply/protocol-concept>. Alternatively, visit [dcricri.org/data-sharing](https://dcricri.org/data-sharing). There may be costs associated with data sharing that researchers would be expected to cover.

## REFERENCES

- Castanheira M, Mendes RE, Jones RN. 2014. Update on Acinetobacter species: mechanisms of antimicrobial resistance and contemporary in vitro activity of minocycline and other treatment options. *Clin Infect Dis* 59(Suppl 6):S367–S373. <https://doi.org/10.1093/cid/ciu706>.
- Chmielarczyk A, Pilarczyk-Żurek M, Kamińska W, Pobjega M, Romaniszyn D, Ziółkowski G, Wójkowska-Mach J, Bulanda M. 2016. Molecular epidemiology and drug resistance of Acinetobacter baumannii isolated from hospitals in southern Poland: ICU as a risk factor for XDR strains. *Microb Drug Resist* 22:328–335. <https://doi.org/10.1089/mdr.2015.0224>.
- Centers for Disease Control and Prevention. 2019. Antibiotic resistance threats in the United States 2019. Centers for Disease Control and Prevention, Atlanta, GA. <https://www.cdc.gov/drugresistance/pdf/threats-report/2019-ar-threats-report-508.pdf>.
- Goff DA, Bauer KA, Mangino JE. 2014. Bad bugs need old drugs: a stewardship program's evaluation of minocycline for multidrug-resistant Acinetobacter baumannii infections. *Clin Infect Dis* 59(Suppl 6):S381–S387. <https://doi.org/10.1093/cid/ciu593>.
- Goff DA, Kaye KS. 2014. Minocycline: an old drug for a new bug: multidrug-resistant Acinetobacter baumannii. *Clin Infect Dis* 59(Suppl 6):S365–S366. <https://doi.org/10.1093/cid/ciu531>.
- Ritchie DJ, Garavaglia-Wilson A. 2014. A review of intravenous minocycline for treatment of multidrug-resistant Acinetobacter infections. *Clin Infect Dis* 59(Suppl 6):S374–S380. <https://doi.org/10.1093/cid/ciu613>.
- Flamm RK, Shortridge D, Castanheira M, Sader HS, Pfaller MA. 2019. *In vitro* activity of minocycline against U.S. isolates of Acinetobacter baumannii-Acinetobacter calcoaceticus species complex, Stenotrophomonas maltophilia, and Burkholderia cepacia complex: results from the SENTRY Antimicrobial Surveillance Program, 2014 to 2018. *Antimicrob Agents Chemother* 63:e01154-19. <https://doi.org/10.1128/AAC.01154-19>.
- Triax Pharmaceuticals, LLC. 2010. Minocycline for injection. Triax Pharmaceuticals, LLC, Cranford, NJ. [https://www.accessdata.fda.gov/drugsatfda\\_docs/label/2010/050444s047lbl.pdf](https://www.accessdata.fda.gov/drugsatfda_docs/label/2010/050444s047lbl.pdf).
- Adibhesami H, Douraghi M, Rahbar M, Abdollahi A. 2015. Minocycline activity against clinical isolates of multidrug-resistant Acinetobacter baumannii. *Clin Microbiol Infect* 21:e79–e80. <https://doi.org/10.1016/j.cmi.2015.07.007>.
- Bowers DR, Cao H, Zhou J, Ledesma KR, Sun D, Lomovskaya O, Tam VH. 2015. Assessment of minocycline and polymyxin B combination against Acinetobacter baumannii. *Antimicrob Agents Chemother* 59:2720–2725. <https://doi.org/10.1128/AAC.04110-14>.
- Welling PG, Shaw WR, Uman SJ, Tse FL, Craig WA. 1975. Pharmacokinetics of minocycline in renal failure. *Antimicrob Agents Chemother* 8:532–537. <https://doi.org/10.1128/aac.8.5.532>.
- Tarazi Z, Sabet M, Dudley MN, Griffith DC. 2019. Pharmacodynamics of minocycline against Acinetobacter baumannii in a rat pneumonia model. *Antimicrob Agents Chemother* 63:e01671-18. <https://doi.org/10.1128/AAC.01671-18>.
- Beal SL. 2001. Ways to fit a PK model with some data below the quantification limit. *J Pharmacokin Pharmacodyn* 28:481–504. <https://doi.org/10.1023/A:1012299115260>.
- Borsuk-De Moor A, Rypulak E, Potręb B, Piwowarczyk P, Borys M, Sysiak J, Onichimowski D, Raszewski G, Czuczwar M, Wiczling P. 2018. Population pharmacokinetics of high-dose tigecycline in patients with sepsis or septic shock. *Antimicrob Agents Chemother* 62:e02273-17. <https://doi.org/10.1128/AAC.02273-17>.
- Fagan SC, Waller JL, Nichols FT, Edwards DJ, Pettigrew LC, Clark WM, Hall CE, Switzer JA, Ergul A, Hess DC. 2010. Minocycline to improve neurologic outcome in stroke (MINOS): a dose-finding study. *Stroke* 41:2283–2287. <https://doi.org/10.1161/STROKEAHA.110.582601>.
- Deitchman AN, Singh RSP, Derendorf H. 2018. Nonlinear protein binding: not what you think. *J Pharm Sci* 107:1754–1760. <https://doi.org/10.1016/j.xphs.2018.03.023>.
- Zhou J, Tran BT, Tam VH. 2017. The complexity of minocycline serum protein binding. *J Antimicrob Chemother* 72:1632–1634. <https://doi.org/10.1093/jac/dkx039>.
- Goldstein A. 1949. The interactions of drugs and plasma proteins. *J Pharmacol Exp Ther* 95(Part 2):102–165.
- Merrikin DJ, Briant J, Rolinson GN. 1983. Effect of protein binding on antibiotic activity in vivo. *J Antimicrob Chemother* 11:233–238. <https://doi.org/10.1093/jac/11.3.233>.
- Liu P, Derendorf H. 2003. Antimicrobial tissue concentrations. *Infect Dis Clin North Am* 17:599–613. [https://doi.org/10.1016/s0891-5520\(03\)00060-6](https://doi.org/10.1016/s0891-5520(03)00060-6).
- Ulldemolins M, Roberts JA, Rello J, Paterson DL, Lipman J. 2011. The effects of hypoalbuminaemia on optimizing antibacterial dosing in critically ill patients. *Clin Pharmacokinet* 50:99–110. <https://doi.org/10.2165/11539220-000000000-00000>.
- Finfer S, Bellomo R, McEvoy S, Lo SK, Myburgh J, Neal B, Norton R, SAFE Study Investigators. 2006. Effect of baseline serum albumin concentration on outcome of resuscitation with albumin or saline in patients in intensive care units: analysis of data from the saline versus albumin fluid evaluation (SAFE) study. *BMJ* 333:1044. <https://doi.org/10.1136/bmj.38985.398704.7C>.
- Fagan SC, Cronin LE, Hess DC. 2011. Minocycline development for acute ischemic stroke. *Transl Stroke Res* 2:202–208. <https://doi.org/10.1007/s12975-011-0072-6>.
- Casha S, Zygun D, McGowan MD, Bains I, Yong VW, Hurlbert RJ. 2012. Results of a phase II placebo-controlled randomized trial of minocycline in acute spinal cord injury. *Brain* 135:1224–1236. <https://doi.org/10.1093/brain/aww072>.
- FDA. 2017. Guidance for industry antibacterial therapies for patients with an unmet medical need for the treatment of serious bacterial diseases. FDA, Silver Spring, MD. <https://www.fda.gov/regulatory-information/search-fda-guidance-documents/antibacterial-therapies-unmet-medical-need-treatment-serious-bacterial-diseases>. Accessed 20 December 2020.
- European Medicines Agency (EMA)—Committee for Medicinal Products for Human Use (CHMP). 2012. Guideline on the evaluation of medicinal products indicated for treatment of bacterial infections (CPMP/EWP/558/95 rev 2). European Medicines Agency, Amsterdam, Netherlands. [https://www.ema.europa.eu/en/documents/scientific-guideline/guideline-evaluation-medicinal-products-indicated-treatment-bacterial-infections-revision-2\\_en.pdf](https://www.ema.europa.eu/en/documents/scientific-guideline/guideline-evaluation-medicinal-products-indicated-treatment-bacterial-infections-revision-2_en.pdf). Accessed 30 May 2019.
- European Medicines Agency (EMA)—Committee for Medicinal Products for Human Use (CHMP). 2016. Guideline on the use of pharmacokinetics and pharmacodynamics in the development of antimicrobial medicinal products (EMA/CHMP/594085/2015). European

- Medicines Agency, Amsterdam, Netherlands. [https://www.ema.europa.eu/en/documents/scientific-guideline/guideline-use-pharmacokinetics-pharmacodynamics-development-antimicrobial-medicinal-products\\_en.pdf](https://www.ema.europa.eu/en/documents/scientific-guideline/guideline-use-pharmacokinetics-pharmacodynamics-development-antimicrobial-medicinal-products_en.pdf). Accessed 30 May 2019.
28. Watanabe A, Anzai Y, Niitsuma K, Saito M, Yanase K, Nakamura M. 2001. Penetration of minocycline hydrochloride into lung tissue and sputum. *Chemotherapy* 47:1–9. <https://doi.org/10.1159/000048494>.
  29. Zhou J, Ledesma KR, Chang K-T, Abodakpi H, Gao S, Tam VH. 2017. Pharmacokinetics and pharmacodynamics of minocycline against *Acinetobacter baumannii* in a neutropenic murine pneumonia model. *Antimicrob Agents Chemother* 61:e02371-16. <https://doi.org/10.1128/AAC.02371-16>.
  30. US Food and Drug Administration. 2020. Antibacterial susceptibility test interpretive criteria. US Food and Drug Administration, Silver Spring, MD. <https://www.fda.gov/drugs/development-resources/antibacterial-susceptibility-test-interpretive-criteria>.
  31. Division of Microbiology and Infectious Diseases (DMID). 19 November 2018. An open-label pharmacokinetic study of minocycline for injection following a single infusion in critically-ill adults (ACUMIN). DMID protocol number 16-0011, version 3.0. Division of Microbiology and Infectious Diseases (DMID), NIAID, NIH, DHHS, Bethesda, MD.
  32. Mager DE, Jusko WJ. 2001. General pharmacokinetic model for drugs exhibiting target-mediated drug disposition. *J Pharmacokinet Pharmacodyn* 28:507–532. <https://doi.org/10.1023/a:1014414520282>.
  33. Mager DE, Krzyzanski W. 2005. Quasi-equilibrium pharmacokinetic model for drugs exhibiting target-mediated drug disposition. *Pharm Res* 22:1589–1596. <https://doi.org/10.1007/s11095-005-6650-0>.
  34. Akaike H. 1979. Bayesian extension of the minimum AIC procedure of autoregressive model fitting. *Biometrika* 66:237–242. <https://doi.org/10.1093/biomet/66.2.237>.
  35. Gehan EA, George SL. 1970. Estimation of human body surface area from height and weight. *Cancer Chemother Rep* 54:225–235.
  36. Bertino JS, Jr. 1993. Measured versus estimated creatinine clearance in patients with low serum creatinine values. *Ann Pharmacother* 27:1439–1442. <https://doi.org/10.1177/106002809302701203>.
  37. Cockcroft DW, Gault MH. 1976. Prediction of creatinine clearance from serum creatinine. *Nephron* 16:31–41. <https://doi.org/10.1159/000180580>.
  38. Smythe M, Hoffman J, Kizy K, Dmuchowski C. 1994. Estimating creatinine clearance in elderly patients with low serum creatinine concentrations. *Am J Hosp Pharm* 51:198–204. <https://doi.org/10.1093/ajhp/51.2.198>.
  39. Borsuk-De Moor A, Rypulak E, Potręć B, Piwowarczyk P, Borys M, Sysiak J, Onichimowski D, Raszewski G, Czuczwar M, Wiczling P. 2018. Population pharmacokinetics of high-dose tigecycline in patients with sepsis or septic shock. *Antimicrob Agents Chemother* 62:e02273-17. <https://doi.org/10.1128/AAC.02273-17>.
  40. Cornely OA, Arenz D, Barraud O, Bayliss M, Dimitriou V, Lovering AM, MacGowan A, Cammarata SK, Fusaro K, Griffith DC, Morgan EE, Loutit JS. 2018. Phase I study to evaluate the safety and pharmacokinetics of single and multiple ascending doses of intravenous minocycline in healthy adult subjects, poster 1387. IDWeek 2018, San Francisco, CA.